

# Localisation in water wave and thin plate problems

Sebastian Rupprecht<sup>1</sup>   Malte A. Peter<sup>1</sup>   Luke G. Bennetts<sup>2</sup>   Hyuck Chung<sup>3</sup>

<sup>1</sup>Institute of Mathematics, University of Augsburg, Germany

<sup>2</sup>School of Mathematics, University of Adelaide, Australia

<sup>3</sup>School of Computer and Mathematical Sciences, Auckland University of Technology, NZ

E-mail addresses: [sebastian.rupprecht@math.uni-augsburg.de](mailto:sebastian.rupprecht@math.uni-augsburg.de), [peter@math.uni-augsburg.de](mailto:peter@math.uni-augsburg.de),  
[luke.bennetts@adelaide.edu.au](mailto:luke.bennetts@adelaide.edu.au), [hchung@aut.ac.nz](mailto:hchung@aut.ac.nz)

## Highlights

- Simulations obtained for water waves over rough seabed and waves in rough in vacuo plate.
- Attenuation rates of effective and individual wave fields extracted, compared and found to differ.

## 1 Introduction

Ocean surface waves attenuate with distance travelled into the sea-ice covered ocean (Meylan et al., 2014). This is reminiscent of the wave localisation phenomenon, which occurs in many branches of wave science. For an incident wave train propagating into a rough (randomly disordered) medium, wave localisation refers to exponential attenuation (on average) of the wave train in the rough medium. (Alternative theories have also been proposed to explain wave attenuation in the ice-covered ocean, e.g. the viscous ice model of Keller, 1998.)

Wave propagation in the ice-covered ocean is conventionally modelled using linear potential-flow theory for the water and thin-plate theory for the ice cover. Bennetts & Peter (2012) conducted a preliminary investigation of wave localisation in the ice-covered ocean due to ice roughness. They modelled the roughness as variations in stiffness and mass of the ice, which are known up to a characteristic length and a root-mean-square amplitude. They extended the multiple-scale method of Mei & Hancock (2003) and Mei et al. (2005) for free-surface waves over a rough seabed to derive a semi-analytic expression for the attenuation rate.

The multiple-scale method is based on the effective wave field, i.e. the mean wave field with respect to realisations of the random medium. Bennetts et al. (2015) showed individual wave fields attenuate far slower than the effective wave field for the rough seabed problem, using large ensembles of numerical solutions for randomly generated realisations of the bed profile.

Here, we extend the study of Bennetts et al. (2015) to problems involving thin plates, with the aim of establishing if effective media theory is

valid to study wave propagation in the ice-covered ocean. We begin by summarising the methods and results of Bennetts et al. (2015) for a rough seabed in intermediate depth. Then, we apply the method to a rough thin plate in vacuo. In both cases, we compare the mean attenuation rates of individual wave fields to the attenuation rates of corresponding effective wave fields.

## 2 Free-surface/rough-bed problem

Let spatial locations in a long transect of the ocean be defined by the Cartesian coordinate system  $(x, z)$ . Horizontal locations are defined by the coordinate  $x$ . Vertical locations are defined by the coordinate  $z$ . The vertical coordinate points upwards and has its origin set to coincide with the equilibrium position of the ocean surface.

Consider a monochromatic wave propagating in the positive  $x$ -direction. The wave amplitude is assumed to be sufficiently small with respect to the wavelength,  $\lambda$ , that linear theory is applicable. In open water, the wavenumber,  $k = 2\pi/\lambda$ , is related to the angular frequency,  $\omega$ , via the dispersion relation  $k \tanh(kh) = K$ , where  $K = \omega^2/g$ ,  $h$  denotes the fluid depth and  $g \approx 9.81 \text{ m s}^{-2}$  denotes acceleration due to gravity.

Consider a seabed that fluctuates about  $z = -\bar{h}$ , where  $\bar{h}$  is an intermediate depth, i.e.  $k\bar{h} = O(1)$ . The fluctuations have a known characteristic length,  $l$ , and root-mean-square amplitude,  $\varepsilon$ , which is also referred to as the roughness amplitude. We assume  $\varepsilon \ll 1$  for consistency with the multiple-scale method although this is not required for a numerical scheme. The function  $z = -h(x)$ , where  $h(x) = \bar{h} - \varepsilon p(x)$  and  $p = O(1)$ , is used to denote the location of the bed.

Under the usual assumptions of linear, time-

harmonic wave theory, the velocity field of water particles in the ocean is defined as the gradient of  $\text{Re}\{(g/i\omega)\phi(x, z)e^{-i\omega t}\}$ . The (complex-valued) velocity potential,  $\phi$ , satisfies Laplace's equation in the undisturbed fluid domain, i.e.

$$\partial_x^2\phi + \partial_z^2\phi = 0 \quad (-h < z < 0). \quad (1a)$$

An impermeability condition is applied on the seabed, i.e.

$$\partial_z\phi + h'(\partial_x\phi) = 0 \quad \text{on } z = -h(x). \quad (1b)$$

The velocity potential is coupled to the wave elevation, denoted  $z = \text{Re}\{\eta(x)e^{-i\omega t}\}$ , via free-surface conditions applied at the equilibrium ocean surface. The free-surface conditions are

$$\phi = \eta \quad \text{and} \quad \partial_z\phi = K\eta \quad \text{on } z = 0, \quad (1c)$$

which are combined into the single condition  $\partial_z\phi = K\phi$  ( $z = 0$ ) for the velocity potential.

Consider the problem in which the roughness extends over a long, finite interval  $x \in (0, L)$ . The bed is otherwise flat and extends to infinity in both positive and negative horizontal directions. A unit-amplitude incident wave is prescribed at  $x \rightarrow -\infty$ . The incident wave is defined by the velocity potential  $\phi = e^{ikx}w(z)$ , where  $w(z) = \cosh\{k(z+h)\}/\cosh(kh)$ . We seek the resulting wave elevation in the interval containing the rough bed.

Let the rough bed profile,  $h(x)$  ( $0 < x < L$ ), be approximated by a piece-wise constant function on  $M$  sub-intervals — the so-called step approximation — and let  $(-\infty, 0)$  and  $(L, \infty)$  be the 0th and  $(M+1)$ th sub-intervals, respectively. We denote the value of the function in the  $m$ th sub-interval as  $h_m$ , and set it to be equal to the value of the continuous bed profile at the mid-point.

In the  $m$ th sub-interval, we have

$$\phi(x, z) = \left( a_m e^{ik_m x} + b_m e^{-ik_m x} \right) w_m(z), \quad (2)$$

where  $k_m$  is the wavenumber for depth  $h_m$  and  $w_m$  is the corresponding vertical mode. The quantities  $a_m$  and  $b_m$  are the wave amplitudes. Incident wave forcing from  $x \rightarrow -\infty$  only is set via  $a_0 = 1$  and  $b_{M+1} = 0$ .

Wave fields in adjacent sub-intervals are related to one another at the interface between the sub-intervals via continuity conditions, which are enforced in a weak sense. An iterative algorithm is used to calculate the amplitudes  $a_m$  ( $m = 1, \dots, M+1$ ) and  $b_m$  ( $m = 0, \dots, M$ ). Bennetts and Squire (2009) give full details of the algorithm. The wave elevation,  $\eta$ , is subsequently recovered via the first component of equation (1c).

Wave elevations are calculated for a large ensemble of randomly generated realisations of the bed profile. The bed profiles share the same amplitude,  $\varepsilon$ , and characteristic length,  $l$ . The relationship between the ensemble of bed profiles is expressed via the autocorrelation condition

$$\langle p(x)p(x-\xi) \rangle = q(|\xi|), \quad (3)$$

where  $\langle \cdot \rangle$  denotes the ensemble average of the included quantity with respect to realisations. We prescribe the Gaussian autocorrelation function  $q(\xi) = e^{-\xi^2/l^2}$ , noting Mei & Hancock (2003) showed an exponential autocorrelation function gives almost identical results. The characteristic length,  $l$ , is hence referred to as the correlation length from here on.

Two measures of the exponential attenuation rate are obtained from the ensemble of wave elevations. First, an attenuation rate,  $Q_{\text{eff}}^{(\text{rs})}$ , is extracted from the effective wave elevation,  $\langle \eta \rangle$ . The attenuation rate, in this case, is defined via

$$|\langle \eta \rangle| \propto e^{-Q_{\text{eff}}^{(\text{rs})}x} \quad (0 < x < L). \quad (4)$$

It is calculated using a least-squares minimisation routine. Second, an attenuation rate,  $Q_{\text{ind}}^{(\text{rs})}$ , is calculated as the ensemble average of attenuation rates of individual wave elevations. The attenuation rate is defined as  $Q_{\text{ind}}^{(\text{rs})} = \langle Q_i \rangle$ , where  $Q_i$  is the attenuation rate extracted from the individual wave elevation  $\eta = \eta_i$ , i.e.

$$|\eta_i| \propto e^{-Q_i x} \quad (0 < x < L). \quad (5)$$

We generate individual realisations of  $p$  using a harmonic random process of the form

$$p(x) = \sqrt{\frac{2}{N}} \sum_{n=1}^N \cos(f_n x + g_n) \quad (N \gg 1). \quad (6)$$

The frequencies  $f_n$  and phases  $g_n$  ( $n = 1, \dots, N$ ) are independently chosen and identically distributed random variables. The standard deviation of the bed profile, with respect to realisations, at all spatial locations  $x$  is normalised to unity. We prescribe probability density functions for frequencies  $f_n$  and phases  $g_n$  ( $n = 1, \dots, N$ ) to satisfy the Gaussian autocorrelation condition (3). The phases are selected from a uniform distribution over the interval  $[0, 2\pi)$ . The frequencies are selected from a Gaussian distribution with zero mean and standard deviation equal to  $\sqrt{2}/l$ .

Fig. 1 shows example individual wave elevations and corresponding effective wave elevations,

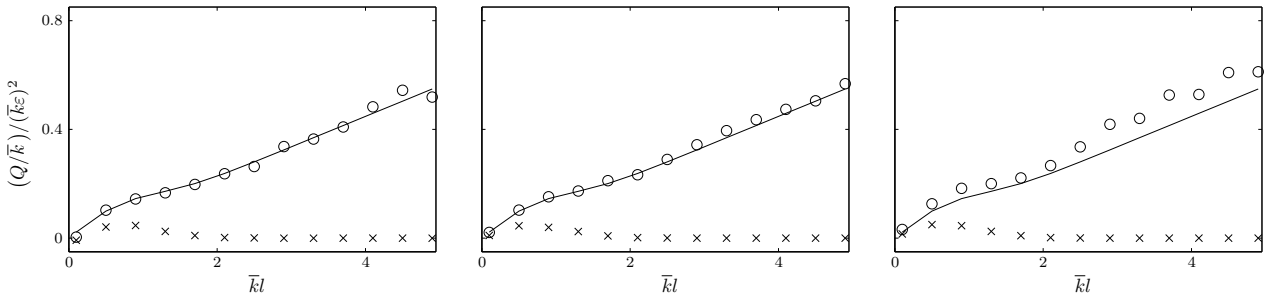


Fig. 2: Attenuation of individual ( $\times$ ) and effective ( $\circ$ ) wave elevations, for  $\bar{k}\varepsilon = 10^{-2}$  (left),  $10^{-1}$  (middle) and  $2 \times 10^{-1}$  (right). Multiple-scale approximation is shown for comparison ( $-$ ).

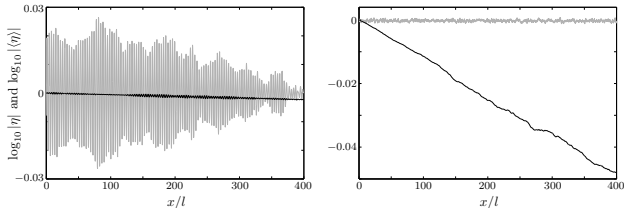


Fig. 1: Example individual wave elevations (grey) and corresponding effective wave elevations (black), for  $\bar{k}\varepsilon = 10^{-2}$  and  $\bar{k}l = 0.9$  (left) and 5 (right).

for a non-dimensional roughness amplitude  $\bar{k}\varepsilon = 10^{-2}$ , and correlation lengths  $\bar{k}l = 0.9$  and 5. The wavenumber  $\bar{k}$  corresponds to the mean depth  $\bar{h}$ , and the intermediate water depth  $\bar{k}\bar{h} = 1$  is set.

The smaller correlation length is chosen to produce visible (although weak) attenuation of the individual wave elevation. The corresponding effective wave elevation attenuates slightly more rapidly than the individual wave elevation.

The largest correlation length is chosen to produce maximal attenuation of the effective wave elevation. The corresponding individual elevation does not attenuate (on the scale shown). Attenuation of the effective elevation is, therefore, not related to the individual elevations.

Fig. 2 shows attenuation rates predicted by the numerical simulations, scaled by  $(\bar{k}\varepsilon)^2$ , as functions of non-dimensional correlation length, for non-dimensional roughness amplitudes  $\bar{k}\varepsilon = 10^{-2}$ ,  $10^{-1}$  and  $2 \times 10^{-1}$ . The multiple-scale approximation (Bennetts et al., 2015) is also shown for comparison.

Attenuation rates of the individual wave elevations have qualitative and quantitative properties markedly different from those of the effective wave elevations. The qualitative behaviour of the attenuation rate of individual wave elevations is intuitive. The attenuation rate is approximately zero (on the linear scale shown) for the smallest non-dimensional correlation length considered,  $\bar{k}l = 0.1$ . In this regime the random bed fluctuations are too rapid to be seen by the waves (ho-

mogenisation limit). The attenuation rate is also approximately zero for correlation lengths greater than two. The roughness in this regime is too mild to modulate the waves. The attenuation rate is only non-zero for correlation lengths between these two regimes, where the roughness is long enough to be seen by the waves and short enough to modulate the waves.

Attenuation of the effective wave elevation is therefore not indicative of attenuation of individual wave elevations for the regime studied. Although the rough seabed forces a random component of the individual wave elevations, the individual wave elevations do not attenuate. We deduce that the dominant source of attenuation of the effective wave elevation is wave cancellation, i.e. decoherence.

### 3 In vacuo plate problem

Next, we consider an infinitely long rough thin plate in vacuo. The problem is one-dimensional in the horizontal coordinate  $x$ . The spatial part  $u(x)$  of the plate deflection  $\text{Re}\{u(x)e^{-i\omega t}\}$  satisfies the thin plate equation

$$\beta \partial_x^4 u - \gamma \omega^2 u = 0 \quad (-\infty < x < \infty), \quad (7)$$

where  $\beta$  is the constant plate stiffness and  $\gamma(x)$  is its varying mass.

With the same step approximation as in the rough-bed problem, the deflection in the  $m$ th sub-interval can be expressed as

$$u(x) = a_m^{(0)} e^{i\kappa_m x} + a_m^{(1)} e^{-\kappa_m x} + b_m^{(0)} e^{-i\kappa_m x} + b_m^{(1)} e^{\kappa_m x}, \quad (8)$$

where the wavenumber  $\kappa_m$  is  $\kappa(x) = (\omega^2 \gamma(x) / \beta)^{1/4}$ , evaluated at the midpoint of the  $m$ th sub-interval. The wave amplitudes  $a_m^{(0)}$  and  $b_m^{(0)}$  correspond to right- and left-travelling waves, respectively, whereas  $a_m^{(1)}$  and  $b_m^{(1)}$  correspond to the evanescent waves, which decay to the right and left, respectively.

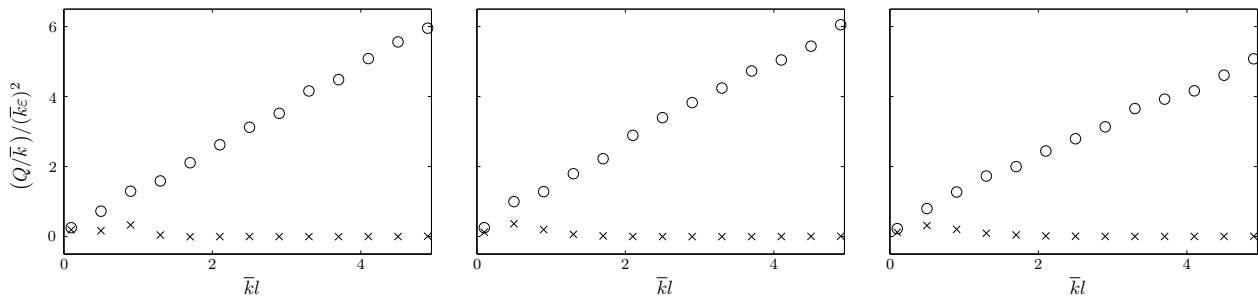


Fig. 4: As in Fig. 2 but for in vacuo plate problem.

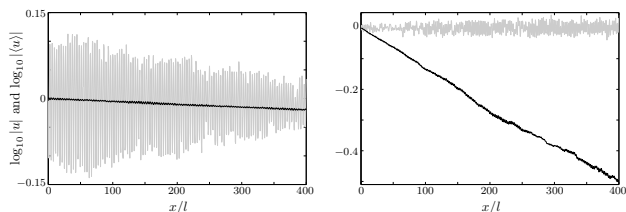


Fig. 3: As in Fig. 1 but for in vacuo plate problem.

The wavenumber is written as  $\kappa(x) = \bar{\kappa} - \varepsilon p(x)$ , where  $\bar{\kappa}$  is its mean. The fluctuation  $p$  is as defined in Section 2.

As for the rough-bed problem, the extent of the plate roughness is restricted to the long finite interval  $x \in (0, L)$ . Outside of this interval, the wavenumber is constant. A unit amplitude wave is incident from  $x \rightarrow -\infty$ .

Wave fields in adjacent sub-intervals are coupled via continuity conditions of displacement, displacement velocity, bending moment and shear stress. An extended version of the iterative algorithm is used to calculate the step approximation for a given realisation of the varying wavenumber, i.e. to calculate the amplitudes  $a_m^{(0)}$ ,  $a_m^{(1)}$  ( $m = 1, \dots, M+1$ ) and  $b_m^{(0)}$ ,  $b_m^{(1)}$  ( $m = 0, \dots, M$ ).

Again, solutions are calculated for large ensembles of different realisations of the varying wavenumber, which share a common correlation length and roughness amplitude. Then, attenuation rates  $Q_{\text{eff}}^{(\text{rs})}$  and  $Q_{\text{ind}}^{(\text{rs})}$ , defined in analogy to the rough bed problem, are extracted.

Figures 3 and 4 show the results for the in vacuo plate, in analogy to figures 1 and 2 for the rough bed, respectively. As can be seen, the behaviour is very similar and the analogous conclusions are drawn.

## 4 Summary and discussion

Numerical results were used to show that, for small-amplitude roughness, individual wave elevations attenuate at a far slower rate than the effective wave elevation for ocean waves travelling over a rough seabed in intermediate depth and also for

waves in a thin plate in vacuo. In particular, in most cases attenuation rates of individual wave elevations are too small for wave localisation to be realised.

It was found that the effective wave elevation attenuates due to wave cancellation in the averaging process. The attenuated wave energy is transferred to the random components of the individual wave fields. Use of the effective wave elevation, therefore, results in misleading predictions of attenuation, and, hence, localisation.

## Acknowledgements

This work was supported by the Group of Eight, Australia, and German Academic Exchange Service (DAAD) Joint Research Co-operation Scheme. LB acknowledges funding support from the Australian Research Council (DE130101571) and the Australian Antarctic Science Grant Program (Project 4123).

## References

- L. G. Bennetts and M. A. Peter, Approximations of wave propagation in one-dimensional multiple scattering problems with random characteristics, In: Proc. 27th IWWFEB (ed. H. B. Bingham et al.), Copenhagen (Denmark), pp. 9–12 (2012).
- L. G. Bennetts, M. A. Peter, and H. Chung, Absence of localisation in ocean wave interactions with a rough seabed in intermediate water depth  $Q$ . *J. Mech. Appl. Math.* (2015), in press.
- L. G. Bennetts and V. A. Squire, Wave scattering by multiple rows of circular ice floes, *J. Fluid Mech.* **639** (2009) 213–238.
- J. B. Keller, Gravity waves on ice covered water, *J. Geophys. Res.* **103** (1998), 7663–7669.
- C. C. Mei and M. J. Hancock, Weakly nonlinear surface waves over a random bed, *J. Fluid Mech.* **475** (2003) 247–268.
- C. C. Mei, M. Stiassnie, and D. K.-P. Yue, *Theory and applications of ocean surface waves. Part I: linear aspects* (World Scientific, 2005).
- M. H. Meylan, L. G. Bennetts, and A. L. Kohout, In-situ measurements and analysis of ocean waves in the Antarctic marginal ice zone *Geophys. Res. Lett.* **14** (2014), 5046–5051.